Abnormal brain activity in rats with sustained hypobaric hypoxia exposure: a resting-state functional magnetic resonance imaging study

Hui Yuan[1,2], Yong Wang[3], Peng-Fei Liu[4], Yun-Long Yue[5], Jin-Song Guo[5], Zhen-Chang Wang[1]

[1]Department of Radiology, Beijing Friendship Hospital, Capital Medical University, Beijing 100050, China;
[2]Department of Radiology, Beijing Shijitan Hospital, Capital Medical University, Beijing 100038, China;
[3]Department of Respiratory and Critical Care Medicine, Hypoxic Laboratory, Beijing Shijitan Hospital, Capital Medical University, Beijing 100038, China;
[4]Department of Anesthesiology, Beijing Shijitan Hospital, Capital Medical University, Beijing 100038, China;
[5]Department of MRI, Beijing Shijitan Hospital, Capital Medical University, Beijing 100038, China.

Abstract

Background: Hypobaric hypoxia (HH) exposure at high altitudes can result in a decline in cognitive function, which may have a serious impact on the daily life of people who migrate to high altitudes. However, the specific HH-induced changes in brain function remain unclear. This study explored changes in brain activity in rats exposed to a sustained HH environment using functional magnetic resonance imaging (fMRI).

Methods: Healthy male rats (8 weeks old) were randomly divided into a model group and a control group. A rat model of cognitive impairment induced by sustained HH exposure was established. The control and model groups completed training and testing in the Morris water maze (MWM). A two-sample *t*-test for between-group difference comparisons was performed. Repeated measures analyses of variance for within-group comparisons were performed and *post-hoc* comparisons were made using the Tukey test. Between-group differences in spontaneous brain activity were assessed using a voxel-wise analysis of resting-state fMRI (rs-fMRI), combined with analyses of the fractional amplitude of low frequency fluctuations (fALFF) in statistical parametric mapping.

Results: In the MWM test, the escape latencies of the model group were significantly longer compared with those of the control group (control group *vs*. model group, day 1: 21.6 ± 3.3 s *vs*. 40.5 ± 3.4 s, $t = -11.282$; day 2: 13.5 ± 2.2 s *vs*. 28.7 ± 5.3 s, $t = -7.492$; day 3: 10.5 ± 2.8 s *vs*. 22.6 ± 6.1 s, $t = -5.099$; day 4: 9.7 ± 2.5 s *vs*. 18.6 ± 5.2 s, $t = -4.363$; day 5: 8.8 ± 2.7 s *vs*. 16.7 ± 5.0 s, $t = -3.932$; all $P < 0.001$). Within both groups, the escape latency at day 5 was significantly shorter than those at other time points (control group: $F = 57.317$, $P < 0.001$; model group: $F = 50.718$, $P < 0.001$). There was no within-group difference in average swimming speed (control group, $F = 1.162$, $P = 0.956$; model group, $F = 0.091$, $P = 0.880$). Within the model group, the time spent within the original platform quadrant was significantly shorter (control group *vs*. model group: 36.1 ± 5.7 s *vs*. 17.8 ± 4.3 s, $t = 7.249$, $P < 0.001$) and the frequency of crossing the original platform quadrant was significantly reduced (control group *vs*. model group: 6.4 ± 1.9 s *vs*. 2.0 ± 0.8 s, $t = 6.037$, $P < 0.001$) compared with the control group. In the rs-fMRI study, compared with the control group, rats in the model group showed widespread reductions in fALFF values throughout the brain.

Conclusions: The abnormalities in spontaneous brain activity indicated by the fALFF measurements may reflect changes in brain function after HH exposure. This widespread abnormal brain activity may help to explain and to provide new insights into the mechanism underlying the impairment of brain function under sustained exposure to high altitudes.

Keywords: Hypobaric hypoxia; Cognition; Magnetic resonance imaging; Functional; Rat

Introduction

Previous studies have shown that conditions of high-altitude hypobaric hypoxia (HH) can diminish brain function in humans and animals, including learning, memory, and other complex information processing functions. The main factors leading to HH-induced changes in cognitive function include oxidative stress and neuronal pathology.[1-5] Magnetic resonance imaging (MRI) has been applied to investigate structural and functional changes in humans exposed to high altitudes, which can enhance our understanding of HH-related cognitive impairment and provide objective indicators for precision medicine. HH has been reported to induce

Access this article online

Quick Response Code:

Website: www.cmj.org

DOI: 10.1097/CM9.0000000000000495

Correspondence to: Prof. Zhen-Chang Wang, Department of Radiology, Beijing Friendship Hospital, Capital Medical University, 95 YongAn Road, Beijing 100050, China
E-Mail: cjr.wzhch@vip.163.com

Chinese Medical Journal 2019;132(21)

Received: 08-05-2019 **Edited by:** Peng Lyu

changes in gray matter volume and white matter fiber bundle function, and has been associated with abnormal activity of functional brain regions.[6-10] Hemosiderin deposits, representative of microhemorrhage, are also observed following HH, which may also contribute to cognitive impairment.[11,12]

Functional magnetic resonance imaging (fMRI) allows for non-invasive evaluations of neural functional changes. Previous fMRI studies investigating HH-induced cognitive changes have primarily focused on the brain function of residents living in or immigrating to high altitudes.[6-8,13] However, it is difficult to avoid the subtle effects of living habits and educational background. The establishment and effective evaluation of animal models of HH-induced cognitive impairment are relatively more objective, have fewer influencing factors, and facilitate the study of subsequent intervention effects.

Therefore, an investigation of brain activity in rats exposed to a sustained HH environment using resting-state fMRI (rs-fMRI) is interesting and essential work. The purpose of our study was to explore the changes in brain activity in rats exposed to a sustained HH environment using fMRI. We hypothesized that there would be altered brain activity in rats with a HH-induced cognitive impairment. These alterations may be based on neuronal damage.

Methods

Ethical approval

This study was approved by the Medical Ethics Committee of Beijing Shijitan Hospital and complied with the Guide for the Care and Use of Laboratory Animals prepared by the Institute of Laboratory Animal Resources and published by the National Institutes of Health.

Animals

Thirty-two healthy male Sprague-Dawley rats (8 weeks old, weighing 280–320 g) were purchased from Beijing Vital River Laboratory Animal Center (Beijing, China; SCXK No. [Beijing] 2016-0006). A randomized, controlled study was conducted on experimental animals reared in the Experimental Animal Center of Beijing Shijitan Hospital.

Housing and grouping

Rats were randomly divided into a model group ($n = 16$) and a control group ($n = 16$). The sample size was estimated according to previously used sample sizes and by following the 3Rs (replacement, reduction, and refinement) principle of experimental animal usage. The model group was housed in an automatically-adjusting HH chamber (Model DF800; Weifang Watson & Company, China), which was maintained at an atmospheric pressure of about 50 kPa and an oxygen concentration of 10%, thus simulating an altitude of 5000 m. The control group was housed under normobaric normoxic conditions in the same room. Rats in both groups were housed four per cage with a 12:12-h light-dark cycle. A pellet diet and water were available *ad libitum*. A temperature of 18 to 25°C and humidity of 55% to 65% were maintained. The chamber and cages were opened every 2 days for cleaning and to resupply food; this procedure lasted 1 h each time. The subsequent experiments were conducted at the end of the 4th week. The duration of sustained HH exposure for the rat model was chosen based on cognitive impairment results resulting from acute and chronic HH exposure in published work.

Morris water maze task

After 4 weeks of HH exposure, eight rats were randomly selected from each of the control and model groups for training and testing in a Morris water maze (MWM) (using X eye MWM; Beijing X eye Scientific Technology Co. Ltd, Beijing, China). The steps were as follows: the water maze was a black circular pool (150 cm in diameter) divided into four equal quadrants. The water temperature was 20 to 22°C, and a circle platform (12 cm in diameter) was placed 1.5 cm beneath the surface of the water as previously described.[14] In the acquisition training, the rats were placed in the water facing the pool wall for each of the four different quadrants in order, and the escape latency and swimming path of the animals as they searched for the platform were recorded using a video camera. During each training, if the hidden platform was not found within 60 s, the escape latency was recorded as 60 s; the rats were then led to the platform and stayed on the platform for 15 s, and then the next quadrant test was performed in order. The training was performed twice per day for 5 successive days. On day 6, the probe test began, in which the platform was removed from the pool to measure spatial learning and memory. We recorded the time spent in the original platform quadrant and the frequency at which the original platform quadrant was crossed during the 60-s probe test.

fMRI acquisition

To minimize the effects of water maze training and normobaric normoxic exposure time after rats were removed from the chamber, MRI was conducted immediately after 4 weeks of HH exposure. That is, another eight rats from each of the model and control groups were randomly selected (16 rats in total) for the MR scanning. Structural and functional images were acquired on a 3T MRI scanner (Ingenia, Philips, the Netherlands) using a standard rat head coil. The rats were anesthetized by intraperitoneal injection of 10% chloral hydrate (3.0 mL/kg) before scanning. They were placed in a prone position and their heads were fixed with a medical band to reduce head movement. Sagittal, coronal, and axial T2-weighted images (T2WI) were acquired using the turbo spin-echo method. Sagittal and coronal T2WI were used to accurately locate the axial image during scanning. The axial T2WI (equivalent to a coronal section of rat brain atlas) was used as a structural image for functional analysis with the following parameters: repetition time (TR) = 3500 ms; echo time (TE) = 80 ms; field of view (FOV) = 60 × 60 mm; flip angle (FA) = 90°; scanning time = 357 s; slice number = 15; slice thickness = 2 mm; layer spacing = 0 mm, number of signal averaged (NSA) = 2. Resting-state functional blood-oxygen-level-dependent images were

acquired using a gradient-echo single-shot echo-planar imaging (EPI) sequence with the following parameters: TR/TE = 2000/22 ms; FOV = 60 × 40 mm; slice number = 25; slice thickness = 1.2 mm; layer spacing = 0 mm; NSA = 1; FA = 90°; dynamics = 120.

Post-processing methods

The data were pre-processed using spmratIHEP,[15,16] based on the statistical parametric mapping (SPM12) software (Wellcome Department of Imaging Science; http://www.fil.ion.ucl.ac.uk/spm) and the rs-fMRI Data Analysis Toolkit (REST) software (http://restfmri.net/forum/index.php?q=rest), and subsequently statistically analyzed using spmratIHEP based on SPM12. All post-processing of the functional images was performed by a single experienced observer who was blinded to the groups. The voxel sizes of all the functional images were first multiplied by a factor of 5 to better approximate human dimensions, which was scaled up in the neuroimaging informatics technology initiative (NIFTI) header. Then, all these functional images were pre-processed using the following main steps: (1) slice timing: the differences of slice acquisition times of each animal were corrected using slice timing; (2) realignment: the temporal processed volumes of each animal were realigned to the first volume to remove any effects of head motion, and a mean image was created. All animals had less than 3 mm of translation in the *x*, *y*, and *z* axes, and less than 1° rotation in each axis; (3) spatial normalization: the realigned volumes were spatially standardized into Paxinos & Watson space by normalizing them with the EPI template using their corresponding mean images. Subsequently, all normalized images were re-sliced as 1.0 mm × 1.5 mm × 1.0 mm voxels (after zooming); (4) smoothing: the normalized functional series were smoothed with a Gaussian kernel of 2 mm^3 full width at half maximum; (5) removal of the linear trend: the smoothed images that had any systematic drift or trend were removed using a linear model; (6) fractional amplitude of low frequency fluctuations (fALFF): the images were used to estimate the value of low frequency fluctuations and then filtered.

Statistical analysis

SPSS software version 23.0 (IBM SPSS Statistics; IBM Corp, Armonk, NY, USA) statistical software was used to analyze the MWM data. A two-sample *t*-test was used to compare data between the model group and control group. Repeated measures analyses of variance were performed separately for the model group and control group using multiple data collected at different times (days 1–5), and *post-hoc* comparisons were performed using the Tukey test. A value of $P < 0.05$ was considered to be statistically significant.

All the fALFF images in Paxinos space were then analyzed voxel-by-voxel based on the framework of the general linear model framework in SPM12. To identify between-group (model group *vs.* control group) differences in fALFF signals, a voxel-wised two-sample *t*-test was performed and an intercranial mask was used. All the voxels with significant fALFF changes were yielded based on a voxel-level height threshold of $P < 0.005$. Then, AlphaSim correction for multiple comparisons was also conducted at the cluster level. Finally, the locations of all significant changes were identified using the Paxinos atlas.

Results

Results of the MWM test

During acquisition training days, escape latencies of the model group were significantly longer compared with those of the control group (control group *vs.* model group, day 1: 21.6 ± 3.3 s *vs.* 40.5 ± 3.4 s, $t = -11.282$; day 2: 13.5 ± 2.2 s *vs.* 28.7 ± 5.3 s, $t = -7.492$; day 3: 10.5 ± 2.8 s *vs.* 22.6 ± 6.1 s, $t = -5.099$; day 4: 9.7 ± 2.5 s *vs.* 18.6 ± 5.2 s, $t = -4.363$; day 5: 8.8 ± 2.7 s *vs.* 16.7 ± 5.0 s, $t = -3.932$; all $P < 0.001$) [Table 1]. Within both groups, the escape latency at day 5 was significantly shorter than those at other time points (control group: $F = 57.317$, $P < 0.001$; model group: $F = 50.718$, $P < 0.001$). There was no within-group difference in average swimming speed (control group: $F = 1.162$, $P = 0.956$; model group: $F = 0.091$, $P = 0.880$). In the probe test, within the model group, the time spent in the original platform quadrant was significantly shorter compared with that in the control group (control group *vs.* model group: 36.1 ± 5.7 s *vs.* 17.8 ± 4.3 s, $t = 7.249$, $P < 0.001$), and the frequency of crossing the original platform quadrant was significantly reduced compared with that in the control group (control group *vs.* model group: 6.4 ± 1.9 s *vs.* 2.0 ± 0.8 s, $t = 6.037$, $P < 0.001$) [Table 2]. The average swimming speed did not significantly differ between the two groups.

Table 1: Five-day acquisition training analysis of escape latency time and average swimming speed of control and model groups.

	Escape latency time (s)				Average swimming speed (mm/s)			
Day	Control group ($n = 8$)	Model group ($n = 8$)	*t*	*P*	Control group ($n = 8$)	Model group ($n = 8$)	*t*	*P*
1	21.6 ± 3.3	40.5 ± 3.4	−11.282	<0.001	140.9 ± 22.4	140.0 ± 20.3	0.094	0.926
2	13.5 ± 2.2	28.7 ± 5.3	−7.492	<0.001	140.9 ± 24.1	142.2 ± 19.8	−0.091	0.929
3	10.5 ± 2.8	22.6 ± 6.1	−5.099	<0.001	140.4 ± 13.2	138.7 ± 11.8	0.160	0.875
4	9.7 ± 2.5	18.6 ± 5.2	−4.363	<0.001	136.9 ± 21.0	140.3 ± 17.5	−0.310	0.761
5	8.8 ± 2.7	16.7 ± 5.0	−3.932	<0.001	141.0 ± 24.1	139.1 ± 16.0	0.196	0.847

Values are presented as mean ± standard deviation. Control group refers to rats reared in normobaric normoxic conditions for 4 weeks; model group refers to rats reared in hypobaric hypoxia conditions for 4 weeks.

Table 2: Probe test analysis of control and model groups.

Effects	Control group ($n = 8$)	Model group ($n = 8$)	t	P
Staying at original platform quadrant time (s)	36.1 ± 5.7	17.8 ± 4.3	7.249	<0.001
Frequency of passing original platform quadrant in 60 s	6.4 ± 1.9	2.0 ± 0.8	6.037	<0.001
Average swimming speed (cm/s)	139.0 ± 22.7	141.0 ± 26.1	−0.164	0.872

Values are presented as mean ± standard deviation. Control group refers to rats reared in normobaric normoxic conditions for 4 weeks; model group refers to rats reared in hypobaric hypoxia conditions for 4 weeks.

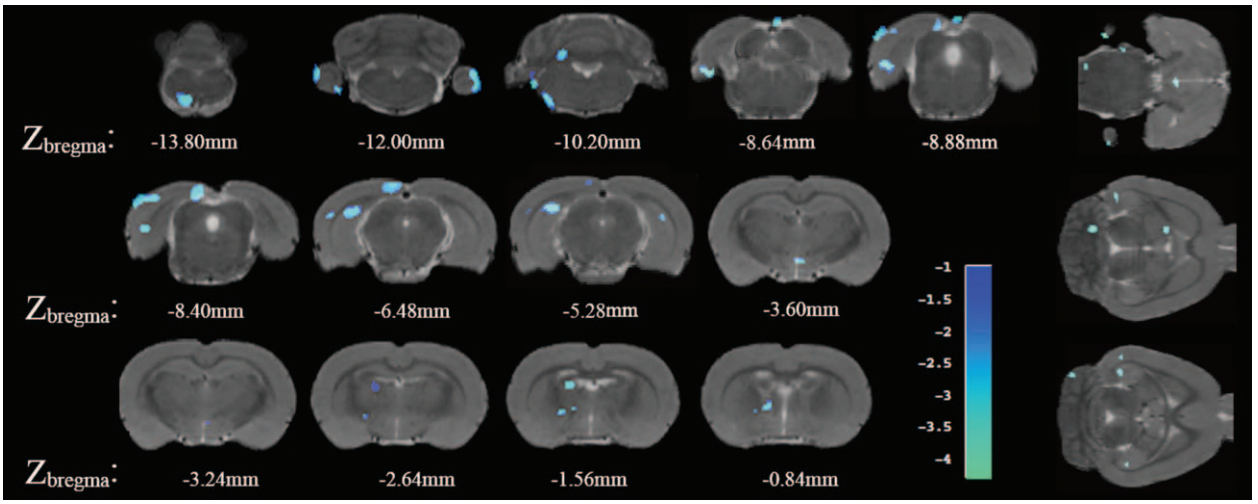

Figure 1: A two-sample *t*-test based on voxel-wise statistical analysis revealed that the inter-group (model group *vs.* control group) differences in fALFF. The blue color regions indicated main fALFF value decreased regions mentioned in Table 3. fALFF: Functional amplitude of low-frequency fluctuations.

fALFF changes in rat brain after HH exposure

A two-sample *t*-test based on voxel-wise statistical analysis revealed that the inter-group (model group *vs.* control group) differences in fALFF were mainly located in the bilateral hippocampus, left entorhinal cortex (EC), bilateral retrosplenial cortex (RSC), left temporal association cortex, left bed nucleus of the stria terminalis, and left optical cortex, left auditory cortex, left septal area, left striatum, left thalamus, bilateral hypothalamus, left pons, left medulla, left cerebellar anterior lobe, and bilateral flocculonodular lobe of the cerebellum. The model group exhibited significantly decreased fALFF in these brain regions compared with the control group [Figure 1 and Table 3].

Discussion

Cognitive impairment in rats after sustained HH exposure

The brain is very sensitive to high altitude hypoxia. It has been shown that HH can shorten escape latency and target quadrant residence time, and reduce the number of crossings of the target quadrant in the MWM, which suggests that spatial learning and memory ability are reduced.[1,3,17] In accordance with previous studies, we found that after 5 days of acquisition training, the ability of all of the rats to locate the platform had improved. However, compared with rats housed in a normobaric normoxia environment, rats exposed to HH for 4 weeks had a significantly longer escape latency ($P < 0.05$), while there was no significant between-group difference in the average swimming speed. This indicated that the model group needed more time to find the platform than the control group, which was suggestive of spatial learning dysfunction rather than physical differences.

The results of the probe test showed that the model group spent significantly less time in the original platform quadrant ($P < 0.05$) and had a significantly lower frequency of crossing the original platform quadrant ($P < 0.05$) than the control group, which indicated spatial memory dysfunction in the model group.

Together, the MWM results revealed the characteristics of spatial cognitive impairment in rats with sustained HH exposure.

Brain activity changes in rats after sustained HH exposure

Learning and memory are important cognitive abilities that involve a complex network of functional brain regions that work together to manage information. The storage and extraction of information involves many brain regions and nerve conduction pathways. In particular, the hippocampus, EC, striatum, thalamus, and basal forebrain play important roles in cognition.[17-20] Although an increasing number of pathophysiological and MRI studies involve the evaluation of brain regions other than just the hippocampus, extensive histological analysis of the whole

Table 3: Brain regions showing significantly decreased fALFF in rats exposed to HH (model group) in comparison with the control group.

Brain regions	Cluster size	*t*	Paxinos & Watson space		
			X	*Y*	*Z*
Left hippocampus	198	−3.4815	−4.0669	2.5862	−6.3579
Left entorhinal cortex	202	−4.1783	−5.7778	4.7005	−8.2779
Left retrosplenial cortex	479	−4.0672	−1.5178	1.0445	−7.0779
Left bed nucleus of stria terminalis	41	−3.6523	−1.7405	5.4266	−0.5979
Left visual cortex	259	−3.3131	−4.8489	1.4994	−7.7979
Left auditory cortex	20	−3.1607	−6.3355	2.9142	−6.5979
Left septal area	50	−3.6628	−2.1315	3.5690	−1.3179
Left striatum	30	−3.3257	−2.8030	5.9915	−1.0779
Left thalamus	39	−3.4340	−3.3459	8.3685	−10.1979
Left mammillary region	23	−3.4646	−0.2341	7.4981	−3.2379
Left pons	235	−3.4340	−3.3459	8.3685	−10.1979
Left medulla oblongata	256	−4.1782	−1.2818	9.0138	−14.5179
Left flocculonodular lobe	226	−4.4092	−7.0647	6.1109	−11.8779
Left anterior lobe of cerebellum	168	−3.9099	−2.1365	4.6840	−10.6779
Right hippocampus	23	−3.2721	5.0142	3.7990	−5.8779
Right retrosplenial cortex	80	−3.1024	0.2229	1.1663	−7.3179
Right mammillary region	21	−3.4646	0.2341	7.4981	−3.2379
Right flocculonodular lobe	92	−3.8891	6.6971	8.0535	−11.6379

Control group refers to rats reared in normobaric normoxic conditions for 4 weeks; model group refers to rats reared in hypobaric hypoxia conditions for 4 weeks. *X*, *Y*, *Z* are the spatial coordinates for the Paxinos & Watson space. *X* represents *X*-axis, which is negative to the left form the midline and positive to the right; *Y* represents *Y*-axis, which is positive to the ventral direction relative to the dorsal; *Z* represents *Z*-axis, which is positive to the olfactory bulb direction relative to the bregma and negative to the cerebellum direction. fALFF: Functional amplitude of low-frequency fluctuations; HH: Hypobaric hypoxia.

brain is unrealistic. Therefore, it is necessary to evaluate changes of cognitive function caused by HH exposure objectively and comprehensively.

The current study is a rare example of an investigation into alterations of local spontaneous neural activity in the rat brain after sustained HH exposure. Analysis combining rs-fMRI with fALFF can measure spontaneous activity of neurons during resting state, and can effectively suppress non-specific signals and reduce interference from physiological noise.[21] This technique is now widely regarded as an important method for measuring local functional activity of the brain. In this study, abnormal brain activity was found in multiple regions of the brain in rats from the model group compared with control group, including the hippocampus, EC, RSC, thalamus, striatum, and cerebellum.

The hippocampus is considered to be an important component of the limbic system and a crucial hub of the default mode network of the brain.[22,23] Studies have shown that hippocampal damage induced by HH tends to be aggravated by increasing altitude and exposure time.[20] Titus *et al*[18] found that the spatial learning of rats exposed to a simulated altitude of 6000 m was slightly affected after 2 days of exposure and significantly impaired after 7 days of exposure; histomorphological studies confirmed that hippocampal injury occurred simultaneously with cognitive impairment. Studies by Maiti *et al*[2,5,24] reported similar findings. In this study, we found that the fALFF in the bilateral hippocampus of the model group was decreased compared with that in the control group, which suggests that HH caused functional impairment in the hippocampus. This impairment may be related to the physiological and pathological changes of hippocampal pyramidal cells and the apoptosis of these cells reported in previous studies.

The EC serves as a gateway for the connection between the hippocampus and neocortex, and plays an important role in advanced cognition, such as spatial learning and memory, spatial exploration, and navigation.[25,26] The EC receives information from the neocortex, and the information is integrated into the place cells of the hippocampus for further processing to facilitate spatial cognition. It has been reported that chronic HH exposure induces a significant decrease of dendritic branching in the EC of rats.[24] However, in the present study, the model group showed a decrease in the fALFF in the left EC, which suggested that the function of the left EC was impaired. This may be related to the impairments in locating the platform and in navigational learning observed in the model group in the MWM.

The RSC, a region that is strongly interconnected with the hippocampal formation, has been shown to play an important role in spatial navigation, learning, and memory, both in humans and in rodents.[25,27] We found that the fALFF was decreased in the RSC of rats in the model group, which is suggestive of cortical functional impairment after HH exposure. However, effects on this brain region have rarely been reported in previous studies of HH rats.

The thalamus, which functions as a relay station of the nervous system, transmits information between different

subcortical regions and the cortex. The mammillary region and the anterior thalamic nucleus play an important role in spatial learning and memory, and it has been shown that injury of the anterior thalamic nucleus leads to more serious spatial memory impairment.[28] The present study found that the fALFF was decreased in the left thalamus and bilateral mammillary regions of rats in the model group, which suggested that dysfunction of these regions may play a role in spatial cognitive impairment in HH.

Previous studies have shown that the striatum is also vulnerable to HH. The apoptosis of striatum was consistent with the damaged hippocampus and cortex under such conditions, which is associated with behavioral impairment in the MWM test.[29] As an important part of the basal forebrain, the septal region has extensive fibrous connections with the hippocampus through the septohippocampal pathway.[30] Some studies have shown that escape latency in the MWM is prolonged and that spatial cognition is impaired in rats with septal area damage.[29] We also found that the fALFF was decreased in the left striatum and the septal region of rats after HH, and that abnormal activation of these brain regions in the model group may be related to changes in cognitive function.

In addition, the fALFF was decreased in some areas of the cerebellum in the model group. In recent years, some studies have reported that the cerebellum is not only responsible for motor coordination, but also participates in some cognitive processes.[30] Rondi-Reig *et al*[31] summarized the current understanding of cerebellar monitoring of sensory information involved in spatial representation and concluded that the cerebellum updates spatial representations by monitoring sensory information and interacting with navigation pathways to maintain a sense of direction and location.[32] However, the abnormal change in this brain region may be due to pathophysiological changes or because of the weakening of the afferent information from the higher cognitive network; we do not know which of these is the case because there is almost no relevant pathophysiological evidence in any relevant studies.

There are also some limitations in this research. First, since MWM training and testing were conducted on rats under normobaric normoxia conditions after 4 weeks of HH exposure in HH-simulated cabin. The MWM and MR scans were performed simultaneously to reduce the impact of normobaric normoxia exposure time on the accuracy of fMRI. Therefore, the correlation analysis between behavior test and fMRI results had no chance to be conducted. The plateau filed experimental study should be done in the future to complement the data. Second, comparing to the control group, there were extensive areas of fALFF reduction but no obvious fALFF increased area was found in the model group, which may cause by neuronal injury or decompensation of the functional brain regions. In further study, multiple model groups with different exposure time (1 day, 7 days, 14 days, and 28 days) should be compared, that continuous observation of spontaneous brain activity may help us to get better understanding of the procedure from compensatory to decompensatory of functional brain areas in model rats.

In conclusion, research of this kind has rarely used rs-fMRI combined with fALFF analysis to observe changes in spontaneous brain activity in rats after sustained HH exposure. Different from relevant previous pathophysiological studies that focused on the hippocampus and local cortex of rats, we found widespread reductions in fALFF throughout the brain. Furthermore, some brain regions with abnormal activation were located at the hub of the default mode network; this finding may provide another key insight into the potential mechanism underlying the cognitive impairment of rats following HH exposure.

Funding

This work was supported by grants from the National Natural Science Foundation of China (No. 61527807) and the Key Program of the National Natural Science Foundation of China (No. 81630003).

Conflicts of interest

None.

References

1. Lefferts WK, DeBlois JP, White CN, Day TA, Heffernan KS, Brutsaert TD. Changes in cognitive function and latent processes of decision-making during incremental ascent to high altitude. Physiol Behav 2019;201:139–145. doi: 10.1016/j.physbeh.2019.01.002.
2. Maiti P, Singh SB, Mallick B, Muthuraju S, Ilavazhagan G. High altitude memory impairment is due to neuronal apoptosis in hippocampus, cortex and striatum. J Chem Neuroanat 2008;36:227–238. doi: 10.1016/j.jchemneu.2008.07.003.
3. Martin K, McLeod E, Périard J, Rattray B, Keegan R, Pyne DB. The impact of environmental stress on cognitive performance: a systematic review. Hum Factors 2019;19:18720819839817. doi: 10.1177/0018720819839817.
4. Bailey DM, Brugniaux JV, Filipponi T, Marley CJ, Stacey B, Soria R, *et al*. Exaggerated systemic oxidative-inflammatory-nitrosative stress in chronic mountain sickness is associated with cognitive decline and depression. J Physiol 2019;597:611–629. doi: 10.1113/JP276898.
5. Maiti P, Singh SB, Muthuraju S, Veleri S, Ilavazhagan G. Hypobaric hypoxia damages the hippocampal pyramidal neurons in the rat brain. Brain Res 2007;1175:1–9. doi: 10.1016/j.brainres.2007.06.106.
6. Zhang J, Chen J, Fan C, Li J, Lin J, Yang T, *et al*. Alteration of spontaneous brain activity after hypoxia-reoxygenation: a resting-state fMRI study. High Alt Med Biol 2017;1:20–26. doi: 10.1089/ham.2016.0083.
7. Chen J, Fan C, Li J, Han Q, Lin J, Yang T, *et al*. Increased intraregional synchronized neural activity in adult brain after prolonged adaptation to high-altitude hypoxia: a resting-state fMRI study. High Alt Med Biol 2016;17:16–24. doi: 10.1089/ham.2015.0104.
8. Chen X, Zhang Q, Wang J, Liu J, Zhang W, Qi S, *et al*. Cognitive and neuroimaging changes in healthy immigrants upon relocation to a high altitude: a panel study. Hum Brain Mapp 2017;38:3865–3877. doi: 10.1002/hbm.23635.
9. Cramer NP, Korotcov A, Bosomtwi A, Xu X, Holman DR, Whiting K, *et al*. Neuronal and vascular deficits following chronic adaptation to high altitude. Exp Neurol 2019;311:293–304. doi: 10.1016/j.expneurol.2018.10.007.
10. Wei W, Wang X, Gong Q, Fan M, Zhang J. Cortical thickness of native tibetans in the Qinghai-tibetan plateau. AJNR Am J Neuroradiol 2017;38:553–560. doi: 10.3174/ajnr.A5050.
11. Hackett PH, Yarnell PR, Weiland DA, Reynard KB. Acute and evolving MRI of high-altitude cerebral edema: microbleeds, edema, and pathophysiology. AJNR Am J Neuroradiol 2019;40:464–469. doi: 10.3174/ajnr.A5897.
12. Chen L, Cai C, Yang T, Lin J, Cai S. Changes in brain iron concentration after exposure to high-altitude hypoxia measured by

quantitative susceptibility mapping. Neuroimage 2017;147:488–499. doi: 10.1016/j.neuroimage.2016.12.033.
13. Chen J, Li J, Han Q, Lin J, Yang T, Chen Z, *et al*. Long-term acclimatization to high-altitude hypoxia modifies interhemispheric functional and structural connectivity in the adult brain. Brain Behav 2016;6:e512. doi: 10.1002/brb3.512.
14. Vorhees CV, Williams MT. Morris water maze: procedures for assessing spatial and related forms of learning and memory. Nat Protoc 2006;1:848–858. doi: 10.1038/nprot.2006.116.
15. Nie B, Chen K, Zhao S, Liu J, Gu X, Yao Q, *et al*. A rat brain MRI template with digital stereotaxic atlas of fine anatomical delineations in paxinos space and its automated application in voxel-wise analysis. Hum Brain Mapp 2013;34:1306–1318. doi: 10.1002/hbm.21511.
16. Nie B, Hui J, Wang L, Chai P, Gao J, Liu S, *et al*. Automatic method for tracing regions of interest in rat brain magnetic resonance imaging studies. J Magn Reson Imaging 2010;32:830–835. doi: 10.1002/jmri.22283.
17. Qaid E, Zakaria R, Sulaiman SF, Yusof NM, Shafin N, Othman Z, *et al*. Insight into potential mechanisms of hypobaric hypoxia–induced learning and memory deficit-lessons from rat studies. Hum Experiment Toxicol 2017;36:1315–1325. doi: 10.1177/0960327116689714.
18. Titus AD, Shankaranarayana RB, Harsha HN, Ramkumar K, Srikumar BN, Singh SB, *et al*. Hypobaric hypoxia-induced dendritic atrophy of hippocampal neurons is associated with cognitive impairment in adult rats. Neuroscience 2007;14:265–278. doi: 10.1016/j.neuroscience.2006.11.037.
19. Zhu M, Xu M, Zhang K, Li J, Ma H, Xia G, *et al*. Effect of acute exposure to hypobaric hypoxia on learning and memory in adult Sprague-Dawley rats. Behav Brain Res 2019;367:82–90. doi: 10.1016/j.bbr.2019.03.047.
20. Ochi G, Yamada Y, Hyodo K, Suwabe K, Fukuie T, Byun K, *et al*. Neural basis for reduced executive performance with hypoxic exercise. NeuroImage 2018;171:75–83. doi: 10.1016/j.neuroimage.2017.12.091.
21. Zou QH, Zhu CZ, Yang Y, Zuo XN, Long XY, Cao QJ, *et al*. An improved approach to detection of amplitude of low-frequency fluctuation (ALFF) for resting-state fMRI: fractional ALFF. J Neurosci Methods 2008;172:137–141. doi: 10.1016/j.jneumeth.2008.04.012.
22. Lisman J, Buzsáki G, Eichenbaum H, Nadel L, Ranganath C, Redish AD. Viewpoints: how the hippocampus contributes to memory, navigation and cognition. Nat Neurosci 2017;20:1434–1447. doi: 10.1038/nn.4661.
23. Eichenbaum H. The role of the hippocampus in navigation is memory. J Neurophysiol 2017;117:1785–1796. doi: 10.1152/jn.00005.2017.
24. Maiti P, Muthuraju S, Ilavazhagan G, Singh SB. Hypobaric hypoxia induces dendritic plasticity in cortical and hippocampal pyramidal neurons in rat brain. Behav Brain Res 2008;189:233–243. doi: 10.1016/j.bbr.2008.01.007.
25. Epstein RA, Patai EZ, Julian JB, Spiers HJ. The cognitive map in humans: spatial navigation and beyond. Nat Neurosci 2017;20:1504–1513. doi: 10.1038/nn.4656.
26. Grieves RM, Duvelle É, Wood ER, Dudchenko PA. Field repetition and local mapping in the hippocampus and the medial entorhinal cortex. J Neurophysiol 2017;118:2378–2388. doi: 10.1152/jn.00933.2016.
27. Ash JA, Lu H, Taxier LR, Long JM, Yang Y, Stein EA, *et al*. Functional connectivity with the retrosplenial cortex predicts cognitive aging in rats. Proc Nat Acad Sci U S A 2016;113:12286–12291. doi: 10.1073/pnas.1525309113.
28. Hwang K, Bertolero MA, Liu WB, D'Esposito M. The human thalamus is an integrative hub for functional brain networks. J Neurosci 2017;37:5594–5607. doi: 10.1523/JNEUROSCI.0067-17.2017.
29. Wu M, Shanabrough M, Leranth C, Alreja M. Cholinergic excitation of septohippocampal GABA but not cholinergic neurons: implications for learning and memory. J Neurosci 2000;20:3900–3908. doi: 10.1523/JNEUROSCI.20-10-03900.2000.
30. Ang ST, Ariffin MZ, Khanna S. The forebrain medial septal region and nociception. Neurobiol Learn Mem 2017;138:238–251. doi: 10.1016/j.nlm.2016.07.017.
31. Rondi-Reig L, Paradis A, Lefort JM, Babayan BM, Tobin C. How the cerebellum may monitor sensory information for spatial representation. Front Sys Neurosci 2014;8:205. doi: 10.3389/fnsys.2014.00205.
32. Schmahmann JD. The cerebellum and cognition. Neurosci Lett 2019;688:62–75. doi: 10.1016/j.neulet.2018.07.005.

How to cite this article: Yuan H, Wang Y, Liu PF, Yue YL, Guo JS, Wang ZC. Abnormal brain activity in rats with sustained hypobaric hypoxia exposure: a resting-state functional magnetic resonance imaging study. Chin Med J 2019;132:2621–2627. doi: 10.1097/CM9.0000000000000495